

Oxygen-Interstitials and Group-V Element Doping for p-Type ZnO

A. M. Gsiea, J. P. Goss, P. R. Briddon, and K. M. Etmimi

Abstract—In realizing devices using ZnO, a key challenge is the production of p-type material. Substitution of oxygen by a group-V impurity is thought to result in deep acceptor levels, but a candidate made up from a complex of a group-V impurity (P, As, Sb) on a Zn site coupled with two vacant Zn sites is widely viewed as a candidate. We show using density-functional simulations that in contrast to such a view, complexes involving oxygen interstitials are energetically more favorable, resulting in group-V impurities coordinated with four, five or six oxygen atoms.

Keywords—DFT, Oxygen, p-Type, ZnO.

I. INTRODUCTION

ZINC-oxide, a transparent semiconductor with a direct, wide band-gap of 3.4 eV and large exciton binding energy of 60 meV, is proposed for applications such as optoelectronic devices, lasers and light emitting diodes [1]–[3]. Perhaps the most significant impediment to the widespread exploitation of ZnO-related materials in electronic and photonic applications is the difficulty in carrier doping, specifically as related to achieving p-type material. Since ZnO exhibits n-type conductivity even without intentional doping, part of difficulty in obtaining p-type conductivity is due to carrier compensation [4].

A potential route is doping with group-V elements, although theoretical studies signified a difficulty to explain the p-type activity for nitrogen at room temperature [5]–[8]. Nevertheless, high hole carrier concentrations have been achieved using N, P, As and Sb [9]–[16].

The conductivity, mobility and charge carrier type is known to depend strongly upon growth conditions including temperature and whether the conditions are zinc or oxygen rich. For example, phosphorus-doped ZnO exhibiting n-type conduction as-grown is converted to p-type by annealing at 600°C in an oxygen atmosphere, [17] and as-grown p-type material is favored in growth involving higher oxygen partial pressure [18].

Quantum-chemical simulations have greatly informed on the potential of candidate dopants to produce p-type ZnO. Some calculations indicate that group-V doping may work [13]–[16], [19], [20]. However, experimentally doping with phosphorus can both produce p-type material or enhance n-type behavior in as-deposited films, indicating the potential for formation of

donor states. This is contrary to the expectation of acceptor-defect formation via substitution on the oxygen site [19].

Where p-type conduction is achieved, one possible shallow acceptor is derived from the triple-donor configuration of P substituting for zinc combined with two zinc-vacancies, [20], [21] since each V_{Zn} is a double acceptor [20]. Such a center would naturally be most favorable in oxygen-rich (zinc-lean) conditions, and suppressed in zinc-rich conditions, leading to a plausible explanation for the efficacy of phosphorus-based p-type doping based on these centers. For group-V elements there is independent experimental evidence that they are more likely to be associated with substitution on the zinc sub-lattice rather than the oxygen sub-lattice, and are more likely to form P–O than P–Zn bonds [22]–[25].

Another native defect yielding a double-acceptor level is interstitial oxygen [26]–[28], O_{int} . This defect also acts as a donor as O_{int} may either be in a non-bonded anion state, or chemically react with the lattice where it forms an O_2 molecule on the O-site depending on charge state. The formation energy of O_{int} is calculated [27], [28] to be comparable or lower than that of V_{Zn} , so it may then be expected to be of importance, especially in oxygen rich conditions.

In this report we present a study of electronic structure, formation energies, and geometries of candidate defects for group-V doped p-type ZnO using first-principles density functional pseudo potential calculations. We show that six-fold coordination with oxygen is considerably more favorable than structures such as $P_{Zn}-(V_{Zn})_2$.

II. METHOD

We use density-functional theory within the AIMPRO package [29], [30]. Defects are simulated within large super-cells containing 192 host-atoms, comprised from $(4 \times 4 \times 3)$ primitive cells. We use the calculated equilibrium lattice constants of $a = 6.18 \text{ \AA}$ and $c = 9.81 \text{ \AA}$, respectively, which are in good agreement with experiment. The Brillouin-zone is sampled using the Monkhorst-Pack [31] scheme with a mesh of $2 \times 2 \times 2$ k -points. Structures are optimized via a conjugate-gradients scheme until the change in energy between iterations is less than 10^{-5} Ha, and forces are below 10^{-3} a.u. Atoms are simulated using *ab initio* pseudo potentials [32] and the total energies and forces are obtained with a local density approximation for the exchange-correlation [33]. The wave functions and charge density are expanded in terms of Gaussian orbitals and plane-waves, respectively [34]. For the Zn, O and group-V impurities we include *s*, *p* and *d* functions, with a total of 28, 28 and 32 functions per atom, respectively. Matrix elements of

A. M. Gsiea is with Faculty of Science, Physics Department, Azzaytuna University, Libya.

J. P. Goss, P. R. Briddon are with the Department of Electrical, Electronic and Computer Engineering, Newcastle Upon Tyne, England.

K. M. Etmimi is with Faculty of Science, Physics Department, Tripoli University, Libya.

Manuscript revised January 11, 2013; revised March 19, 2013.

the Hamiltonian are determined using a plane wave expansion of the density and Kohn-Sham potential [35] with a cutoff of 150 Ry, yielding well converged total energies with respect to the charge density basis.

We calculate the formation energy of a defect X using

$$E^f(X, q) = E^{\text{tot}}(X, q) - \sum_i \mu_i + q\mu_e + \chi(X, q) \quad (1)$$

where $E^{\text{tot}}(X, q)$ is the total energy of system X in charge state q . μ_i denotes the chemical potential of atomic species, $E_v(X, q)$ is the Fermi energy at the valence-band top, μ_e is the electron chemical potential, defined as zero at the valence band top, and $\chi(X, q)$ is a correction term to compensate for artifacts of the boundary conditions. In ZnO, the chemical potentials of components μ_{O} and μ_{Zn} are related by $E(\text{ZnO}) = \mu_{\text{O}} + \mu_{\text{Zn}}$ where $E(\text{ZnO})$ is the energy per bulk formula unit in ZnO. The range of possible values for μ_{O} and μ_{Zn} is related to the requirement for ZnO to be stable relative to decomposition into its elemental constituents, so that the zinc-rich limit is taken from zinc-metal, and for oxygen-rich limit μ_{O} is taken from the O_2 molecule. The heat of formation for ZnO in this way is calculated to be 3.9 eV, while experimentally it is 3.61 eV [36]. Relative formation energies *per impurity atom* are independent of the impurity chemical potential, but for the reference state of phosphorus-based centers shown in Figs. 2, 7, and 8, μ_{P} is derived by comparison with P_4O_6 , and is therefore linked to μ_{O} .

For the electrical characteristics of the defect centers, we calculate the transition levels, $E(q, q')$, defined as the electron chemical potential where the formation energies for two charge states, q and q' , are equal. The effect upon the electrical levels arising from the periodic boundary condition, $\chi(X, q)$ in Eq. 1, is a complicated and controversial quantity to estimate. In this study, we have adopted a simple approach as we are focusing on the larger differences between the formation energies of different structures, rather than the specific values of the donor and acceptor levels. We correct the total energies using the Lany and Zunger model [37], and to take into account the underestimation of the band gap we also add a term proportional to the number of electrons in a conduction-band-like level [21], [28] of 2 eV per electron arising from a simple addition of the difference between the calculated and experimental band-gaps. The calculated electrical levels should be regarded as having error bars due to uncertainties in the calculation of the energies and correction terms of the order of a few 10ths of an eV.

When comparing the absolute formation energies, and in particular in the important cases of comparison between like-systems, such as band-like donors, or comparison between the models for p-type doping, the corrections largely cancel. Then the energy differences between two donor systems, or two acceptor systems are generally accepted to be reasonably reliable at a quantitative level.

III. RESULTS

We find strong trends for group-V elements [38]. Therefore we illustrate our results in detail only for phosphorus, starting

with P substituting for oxygen (P_{O}).

A. Phosphorus substituting for oxygen

We examined P on the O-site (P_{O}). The structure obtained for neutral P_{O} is shown in Fig. 1(a). The P atom remains on-site and is approximately tetrahedral with four P–Zn bonds of 2.23–2.27 Å, in excellent agreement with previous calculations [21]. Since P has one fewer valence electron than the oxygen atom it replaces, it is expected that P_{O} will be an acceptor, and indeed this is what we find. The negative charged state closely resembles the neutral in structure, but with slightly shorter P–Zn bonds of 2.17–2.20 Å, also in excellent agreement with previous calculations [6]. The charge-dependent formation energies (Fig. 2) indicates a $(-)/0$ acceptor level around $E_v + 1.0$ eV, far too deep for p-type doping. In line with the consistency found with the literature for the structural results, this calculated electrical level broadly agrees with previous theory [6], [21], [39], [40].

In addition, P_{O} may act as a donor, as it can undergo a chemical reaction with a neighboring oxygen atom, forming the structure shown schematically in Fig. 1(b), the so-called AX center [6]. Indeed, in this form our calculations suggest that P_{O} may donate *two* electrons. As ZnO is a hexagonal material, there are three distinct types of second-neighbor sites by symmetry. The orientation for the AX^{+1} structure which we find to be lowest in energy is differs from that more previously suggested [41], which we find is meta-stable and 0.5 eV, higher in energy. In addition, there is a meta-stable, on-site form in the positive charge state which is around 1.0 eV higher in energy than AX^{+1} . The AX structure is metastable in the neutral charge state, but has a formation energy around 2.6 eV *higher* than that of the on-site form. In all charge states, where present, the substantial structural re-arrangement can be viewed as the formation of a P=O molecular fragment within the ZnO lattice, and the band-gap levels are highly characteristic of π^* -interactions between the two atoms.

The existence of the AX form introduces the possibility of a $(-)/+$ transition from the on-site negative charge state to the AX positively charged configuration. We find that this level lies around $E_v + 1.3$ eV. A second donor level is found at $E_v + 0.9$ eV, which can be understood as further depopulation of a π^* combination of orbitals on the P=O pair.

This picture is extended when we examine the possibility of P_{O} forming pairs. We have simulated P pairs in a number of starting configurations reflecting the anisotropy of the lattice. Where P_{O} pairs are in the nearest-neighbor configuration, there is a *spontaneous* reconstruction between the P atoms to form a P_2 molecule, with the more energetically favorable orientation combining O-sites in different basal planes, as shown in Fig. 1(c). This significantly reduces the formation energy (Fig. 2) for substitution onto the oxygen lattice, the formation energy *per P atom* being 1.3 eV lower for the pair as compared with isolated P_{O} centers. It is clear that P_{O} -pairs have a structure which strongly resembles the P_{O} AX center.

One might expect P_{O} -pairs to preferentially adopt a different structure if they become negatively charged, since individually P_{O} centers in the negative charge state are close to tetrahedral

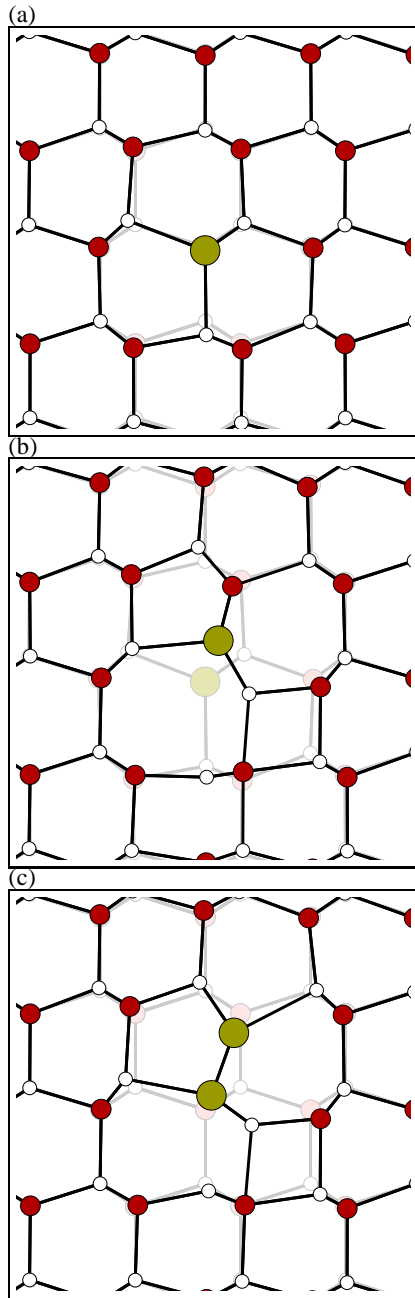


Fig. 1. Projections onto (0110) of the structure of P_O in (a) the neutral charge state and (b) the positive charge state, AX structure. (c) shows the lowest energy orientation of the reconstructed P_O -pair. Small, medium, and large circles represent Zn, O, and P atoms, respectively. In (a) and (c) the host-lattice is shown in the background as a reference, whereas in (b) the on-site structure is shown in the background to help show the sense of the reconstruction. The c -axis is in the vertical direction in the projections.

and on-site. Perhaps surprisingly, the reconstruction between P atoms is *not* lost upon charging with additional electrons, and we conclude that the energy gained in the formation of the P–P bond destabilizes the neighboring on-site P_O -pairs, *even if they are negatively charged*, and the electrons are moved into the host conduction band. Thus, we find that nearest-neighbor P_O -

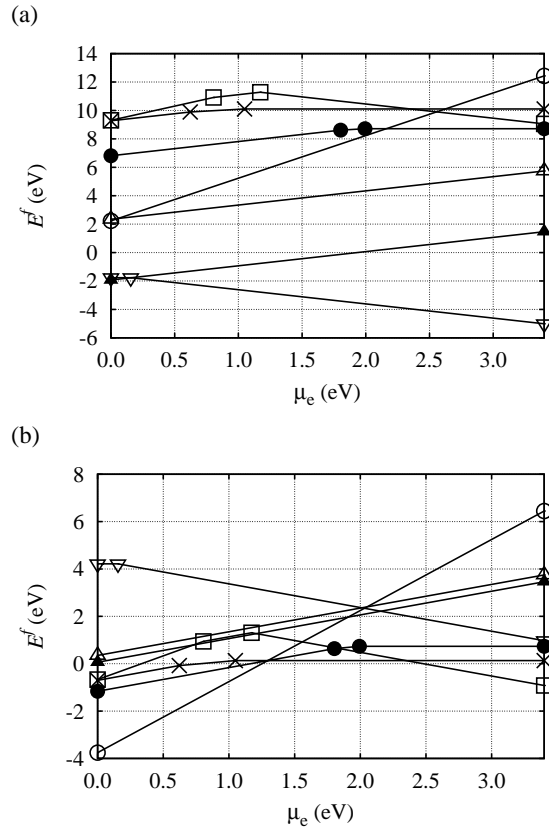


Fig. 2. Plot of E^f vs. μ_e for key P-containing defects associated with the oxygen-lattice in ZnO. All energies are calculated using the 192 atom supercell: P_O (\square), $(P_O)_2$ (\times), $(P_2)_O$ (\bullet), $(P_O)_O$ (\circ), $(PO_2)_O$ (Δ), $(PO_3)_O$ (\blacktriangle), and $(PO_4)_O$ (∇). (a) Oxygen-rich conditions and (b) zinc-rich conditions.

pairs cannot act as acceptors. There are $(0/+)$ and $(+/2+)$ levels in the band-gap, estimated at $E_v + 1.1$ eV and $E_v + 0.7$ eV, respectively (Fig. 2). In equilibrium, therefore, if P_O are significant in the manufacture of p-type ZnO, they will have to compete with the formation of $(P_O)_2$ double-donors.

The formation of P–O reconstructions in the positive charge state of P_O , and the P–P bond in neighboring P_O -pairs reflects the impact that the formation of strong, covalent bonds has upon the total energies. We shall show that this is a driving factor in a wide range of P-containing centers associated with both the oxygen and zinc lattices.

B. Interstitial P

We have also examined the possibility for phosphorus to lie in an interstitial site (P_i). Since such defect spontaneously react with the oxygen in the lattice, interstitial P can be thought of as being associated with the oxygen lattice, so we examine them here.

There is a significant number of metastable P_i structures, separated by small differences in total energy, but chemically distinct with differing numbers and orientation of P–O (and P–Zn) bonds. In general they are characterized by the phosphorus being covalently bonded to one, two, or three host oxygen

atoms, and two characteristic structures that we found are illustrated in Fig. 3.

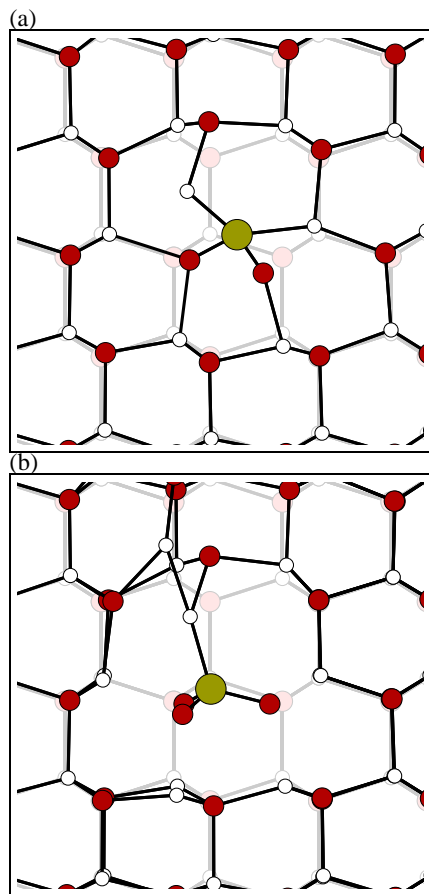


Fig. 3. Schematic of the most stable P_i structure. Colors and axes are as in Fig. 1.

P_i behaves as a *triple donor*, with a $(0/+3)$ transition around $E_v + 2.3$ eV. The localization of the band-gap levels of P_i suggest that it can be characterized as a molecular ion, in this case PO_2 and PO_3 .

We have examined the energy barrier for diffusion. The profile is shown in Fig. 4, which includes many stages, such as bond-rotations, and inter-conversion between PO_2 and $P=O$ molecular fragments. The details of the path are less important than the rate-limiting barrier, which is about 1 eV. This must be an upper limit to the net barrier height (there may be other, lower energy routes) so at growth temperatures, where such a barrier would be easily overcome, P_i is a relatively mobile species.

We calculate a formation energy of P_i of 4.8–5.9 eV, (the range of values arising due to the dependence of μ_P upon μ_O), so that even in the most favorable growth conditions the likelihood of formation of this center is rather low.

In addition, during the simulations of P_i we observed *spontaneous* reactions of the type $P_i \rightarrow P_{Zn} + Zn_i$. Using the formation energies of P_i and the reaction products separated from each other, we calculate the loss of P_i and formation of

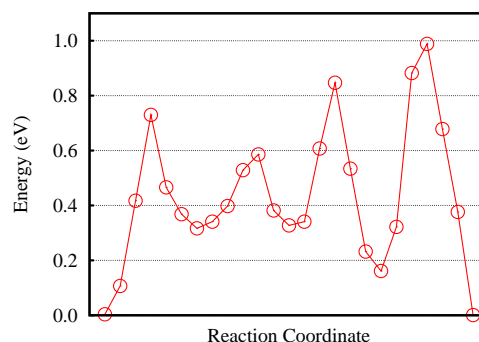


Fig. 4. NEB calculated migration barrier for interstitial phosphorus in ZnO.

Zn_i in the neutral charge state involves no significant gain or loss in energy.

We note that substitution of oxygen by a P_2 molecule can be thought of as P_O capturing a phosphorus interstitial, and such centers have been proposed as possessing a low formation-energy previously [21] in p-type material. Fig. 2 includes such a center, which is competitive in energy in p-type material, but is never the most stable form of P-center associated with the oxygen sub-lattice.

C. Phosphate ion on the oxygen lattice

The structure and chemistry of P_i is suggestive of a class of defects which are P-containing molecules substituting for O, $(PO_n)_O$. For $n = 4$, this represents a phosphate ion at the oxygen site. The structure is shown schematically in Fig. 5. The phosphate group normally adopts a -3 oxidation state, rather than the -2 oxidation state of the oxygen ion it replaces. This leads to a deficit of charge at this defect site, and it acts as an effective acceptor. The band-structure for the neutral charge state is shown in Fig. 5(b), indicating a shallow acceptor level, and the charge-state dependent formation energies indicate a level at $E_v + 0.2$ eV.

This defect contains additional oxygen atoms relative to the host, and is therefore clearly a center that will be favored energetically under oxygen-rich growth conditions. The absolute formation energy of this shallow acceptor in the oxygen-rich limit is found to be highly favorable in comparison to other acceptor structures.

We find that the intermediates (in terms of increasing oxygen content) between P_i and $(PO_4)_O$ all act as donors, but are energetically less favorable than the phosphate ion in oxygen-rich conditions. However, there is a strong theme in terms of the structures. For example, in the $(PO_3)_O$ center, phosphorus forms an additional bond to a neighboring O-site, and can be considered to be a phosphate ion distributed over two host O-sites. Since the phosphate ion normally adopts a -3 charge state, which in this case is substituting for two O^{-2} ions, it is easy to see why $(PO_3)_O$ acts as a single donor.

$(PO_n)_O$ centers are included in Fig. 2 for comparison with other defects associated with the oxygen sub-lattice, and in the oxygen rich limit, these centers are highly favorable on

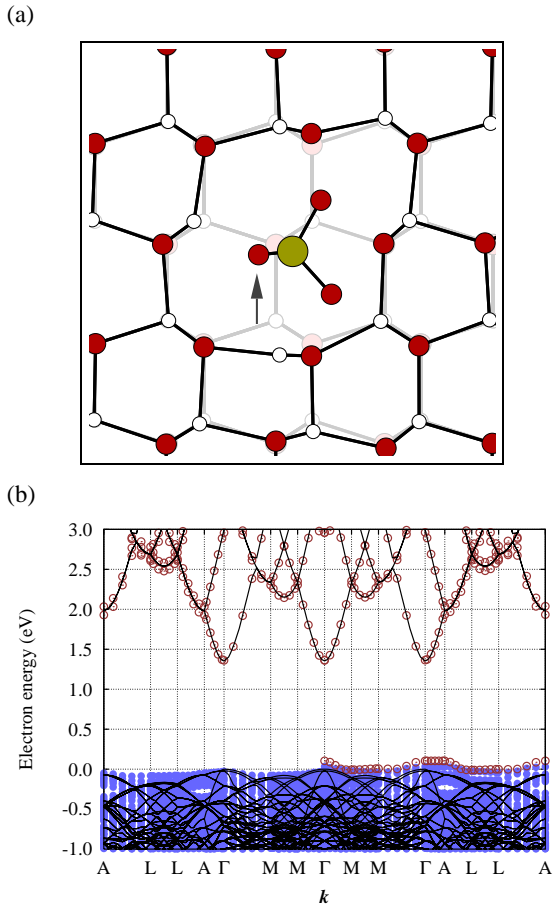


Fig. 5. (a) Schematic of a phosphate ion at an oxygen site. Symbols are as in Fig. 1, and arrow indicates where one of the O-atoms in the phosphate ion eclipses another. (b) The Kohn-Sham band-structure for this center. Black lines represent the host bands of a defect free cell of the same size. Filled and empty circles show occupied and unoccupied bands of $(\text{PO}_4)_\text{O}$, with the bands to the right of center being the spin-down states, and to the left spin-up. Only bands in the vicinity of the band-gap are shown, and the bands are set such that the valence band top is at zero.

the basis of formation energy. We shall return to this point in Sec. III-F.

D. Phosphorus substituting for zinc

We now move to P on the zinc lattice. These centers, with the exceptions highlighted here, have received relatively little attention in the literature, but we shall show that they are probably of greater relevance than P on the oxygen lattice.

Since phosphorus has three more valence electrons than Zn, P_{Zn} is expected to be a triple donor. The relaxed geometry, shown schematically in Fig. 6(a) indicates a significant dilation of the surrounding Zn–O bonds, and it is more realistic to describe the P_{Zn} as PO_4 inside a cavity bordered immediately by 12 Zn^{+2} sites. As noted above, the phosphate group normally exists in the -3 oxidation state, and the twelve Zn atoms surrounding PO_4 readily provide these electrons. However, since each Zn-neighbor has $1/2$ an electron to donate, there are a further three electrons to be accounted for.

In our calculations these go to the host conduction band, so that in effect the phosphate group in ZnO is a shallow triple donor (Fig. 7). The $(0/+1)$ and $(+1/+2)$ levels lie above the conduction-band minimum, and only the $+3$ charge state is thermodynamically stable. Thus, as previously suggested [21], we find P_{Zn} is expected to lead to n-type conduction.

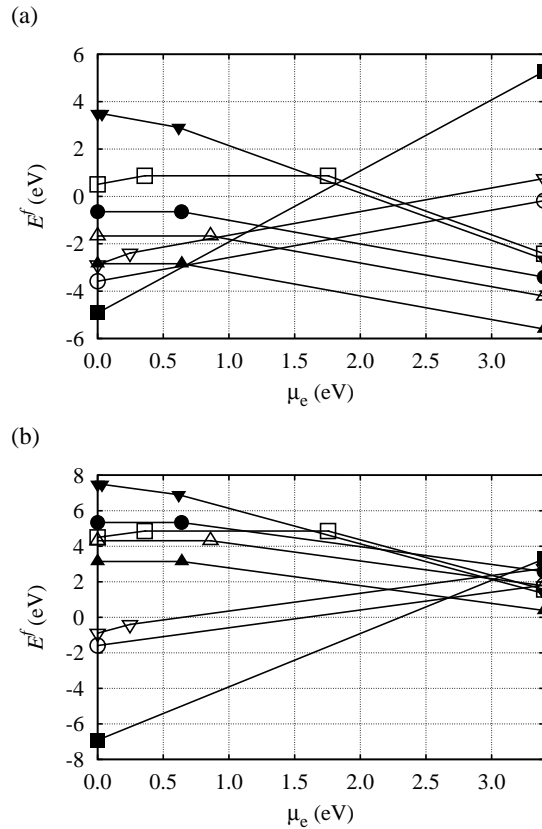


Fig. 7. Plot of E^f vs. μ_e for key P-containing defects associated with the zinc sub-lattice in ZnO calculated using the 192 atom supercell: V_{Zn} (\blacktriangledown), O_{int} (\square), P_{Zn} (\blacksquare), $\text{P}_{\text{Zn}}-\text{V}_{\text{Zn}}$ (∇), $\text{P}_{\text{Zn}}-\text{O}_{\text{int}}$ (\circ), $\text{P}_{\text{Zn}}-(\text{V}_{\text{Zn}})_2$ (\bullet), $\text{P}_{\text{Zn}}-\text{V}_{\text{Zn}}-\text{O}_{\text{int}}$ (\triangle), and $\text{P}_{\text{Zn}}-(\text{O}_{\text{int}})_2$ (\blacktriangle). (a) Oxygen-rich conditions and (b) zinc-rich conditions.

As with P_{O} , to support the use of a 192-atom cell we also simulated P_{Zn} in a 400 atom cell ($5 \times 5 \times 4$ primitive unit cells). The formation energy and electrical levels are in close agreement between these cells, from which we conclude that the 192-atom supercell is adequate.

E. P_{Zn} complexes with V_{Zn} and O_{int}

As P_{Zn} is a triple donor, it is expected to be a single donor when in complexes with V_{Zn} or O_{int} which both have the capacity to act as double acceptors. Our analysis confirms this, with the donor levels of both $\text{P}_{\text{Zn}}-\text{V}_{\text{Zn}}$ and $\text{P}_{\text{Zn}}-\text{O}_{\text{int}}$ complexes predicted to lie above E_c (∇ and \circ in Fig. 7). Fig. 7 also shows that $\text{P}_{\text{Zn}}-\text{O}_{\text{int}}$ is thermodynamically more stable than $\text{P}_{\text{Zn}}-\text{V}_{\text{Zn}}$ independent of whether the material is in the oxygen-rich or zinc-rich regimes [42]. $\text{P}_{\text{Zn}}-\text{O}_{\text{int}}$ [Fig. 6(c)] can be described as P_{Zn} in five-fold coordination with oxygen,

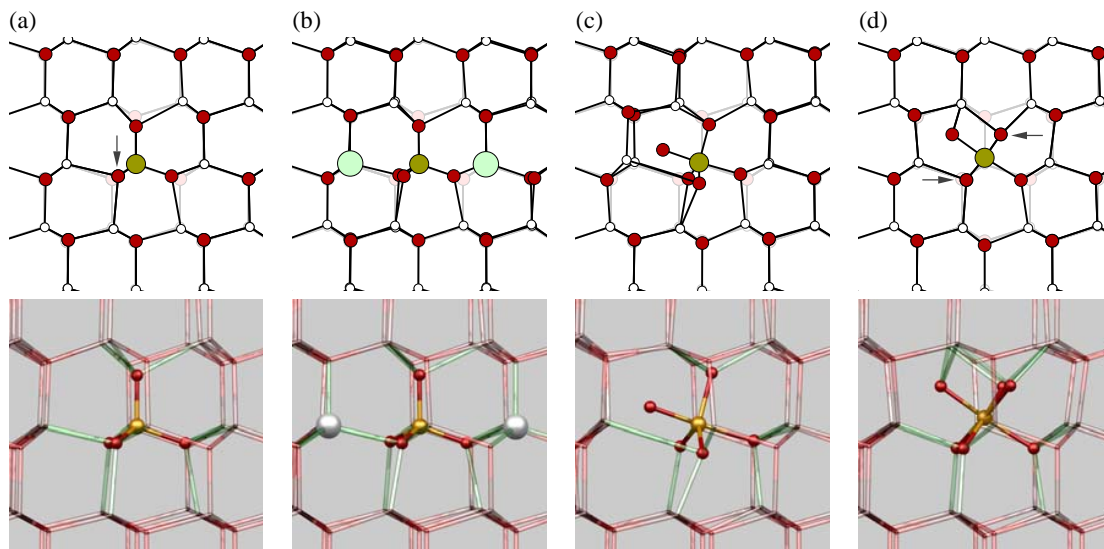


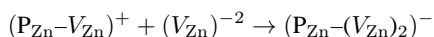
Fig. 6. Projections of the structures of P_{Zn} -related defects in ZnO, following specifications of Fig. 1. In addition for each structure a perspective view is presented with the central atom being P, with the other smaller atoms oxygen and the large spheres representing V_{Zn} . (a) P_{Zn} , (b) $P_{Zn}-(V_{Zn})_2$, (c) $P_{Zn}-O_{int}$, and (d) $P_{Zn}-(O_{int})_2$.

i. e. somewhat akin to a phosphorane, further indicating the significance of the stabilizing effect in the formation of P–O bonds.

Since $P_{Zn}-O_{int}$ and $P_{Zn}-V_{Zn}$ are single donors, they may in turn be converted into acceptors by the addition of an additional V_{Zn} or O_{int} center. Such a procedure results in three types of p-type structure.

The first is the well established complex with two V_{Zn} sites [20], [21], $P_{Zn}-(V_{Zn})_2$. This is stabilized by the attractive Coulomb interaction between the components.

Due to the number of components and the anisotropy of the lattice, there are many possible $P_{Zn}-(V_{Zn})_2$ orientations determined by the V_{Zn} positions relative to P_{Zn} . The most stable structure we find is shown in Fig. 6(b), but in other orientation where the vacancies are in the nearest shell of Zn-neighbors to the P-site, the total energies vary by just 100s of meV. The structure we find to be most stable is 35 meV, lower than that previously suggested using smaller simulation cells [21]. We calculate the binding energy of the complex relative to separate $P_{Zn}-V_{Zn}$ and V_{Zn} centers is 3.7 eV for all species in the neutral charge state, and 1.3 eV for the reaction



both in good agreement with previous calculations [21], [43]. The formation energies for the various charge states of the most stable stable orientation is plotted in Fig. 7, showing that the acceptor level at around $E_v + 0.6$ eV, which is in good agreement with previous calculations [21]. Although there is some uncertainty in this estimate, such a deep level would not be result in efficient p-type doping, and these centers are therefore predicted to be less effective than $(PO_4)_O$.

The second complex configuration is $P_{Zn}-V_{Zn}-O_{int}$. Among the stable structures, one is where phosphorus is bounded to five oxygen neighbors, somewhat similar to the structure

is illustrated in Fig. 6(c), but with one neighboring Zn site replaced by V_{Zn} . However, an alternative structure where the O_{int} component becomes detached from the P center resulting in a phosphate structure P_{Zn} in close proximity with V_{Zn} and O_{int} is around 0.4 eV lower in energy in both the neutral and negative charge states. This difference in energy are nearly independent of charge state, with all low-energy structures we examined resulting in a deep acceptor level (Fig. 7).

Since $P_{Zn}-O_{int}$ is more stable than $P_{Zn}-V_{Zn}$, one might anticipate that $P_{Zn}-V_{Zn}-O_{int}$ will be more stable than $P_{Zn}-(V_{Zn})_2$, and this is precisely what we find. The formation energies in the neutral charge state in Fig. 7 illustrates this difference, which is independent of μ_O and estimated at 0.6 eV.

The final configuration is $P_{Zn}-(O_{int})_2$. By examination of the relaxed geometry it is clear that it is more realistic to describe the system not as $P_{Zn}-(O_{int})_2$, but as a PO_6 molecular group in a cage surrounded by 12 Zn sites, as illustrated in Fig. 6(d). The calculations show that this is the most stable structure for the candidates we have examined for p-type ZnO with phosphorus. In addition, due to the relative formation energies of V_{Zn} and O_{int} , it has a favorable binding energy of 2.4 eV per O_{int} under a reaction resulting in dissociation into $P_{Zn}-O_{int}$ and O_{int} species in the neutral charge state. As with $P_{Zn}-(V_{Zn})_2$ and $P_{Zn}-V_{Zn}-O_{int}$, the calculated acceptor level is relatively deep. However, again we note that the methodology leads to appreciable uncertainty in the precise location of the acceptor level, and whether or not any of these complexes may lead to p-type conductivity remains to be established.

It is perhaps worth noting that five-fold (phosphoranes) and six-fold coordinated phosphorus compounds have been reported both experimentally and theoretically [44], [45]. Indeed, the P–O bond-lengths and angles in the point-defects above are close to the experimental values for P co-ordinated

with five oxygen atoms in organic compounds [46], providing some additional confidence in the chemically sound nature of the structures we have obtained.

F. Discussion and chemical trends

Of the phosphorus-containing centers discussed in this paper, many act as shallow donors, and others possible acceptors. To establish a model of the equilibrium behavior of P-doped ZnO, we compare their total formation energies as a function of the growth conditions (O-rich vs. Zn-rich) and the electron chemical potential.

In O-rich conditions, Fig. 8(a), substitution of P onto the Zn-lattice is highly favorable and the possible acceptor complexes are favored for most values of μ_e . However in p-type material, P_{Zn} is favored, so in equilibrium a combination of the two species would form. A key result is that under O-rich conditions it is not $P_{Zn}-(V_{Zn})_2$ but $P_{Zn}-(O_{int})_2$ that is lowest in energy, and given the uncertainty in the precise location of the acceptor level, it must be viewed as a candidate for the formation of p-type ZnO.

Experimentally, p-type P-doped ZnO has been reported with an acceptor level located at 127 meV above the valence band [47]. In XPS, the general view is that in p-type material the group-V elements are bonded to oxygen [48]. However, XANES data [49] might be suggestive of P on the O-site, as the data is interpreted as P existing in the -3 oxidation state in p-type material, possibly consistent with P_O .

For Zn-rich material the $P_{Zn}-(O_{int})_2$ is less favorable than donor structures, with the uptake of P expected to be dominated by the incorporation of P_{Zn} .

What is the origin of the stability of these configurations? The formation of PO_n , $n = 1-6$, molecular fragments in the highly stable configurations reflects the relative strength of the bonding between P and O, relative to P and Zn. Despite the relative cost in formation of O_{int} , the formation of P-O bonds significantly stabilizes them. Indeed, the formation of octahedrally bonded P and As is established under high-pressures in minerals. [50]–[54]

Combining the most stable forms of P-containing centers, Fig. 8 shows that in both oxygen and zinc rich conditions, there is a definite driving force for the formation of complexes where P-O bonds are formed. The phosphate ion on either lattice is low in energy, and can move the Fermi-level towards either the valence band top or the conduction band minimum. Additional oxygen atoms can be introduced in the presence of P, such as the highly stable $P_{Zn}-(O_{int})_2$ center. Under no conditions are P-Zn bonds favored (such as might occur in P_O).

Guided by the results for P, we have also examined the relative energies of candidate acceptor species based upon As and Sb [55]. The general trends are mostly *independent of chemical species* and in fact we find similarities in the formation of six-fold coordination for chalcogens substituting for Zn. Table I summarizes these results. The generality of O_{int} -based centers being energetically favored is clear, and has widespread implications for understanding the properties these impurities.

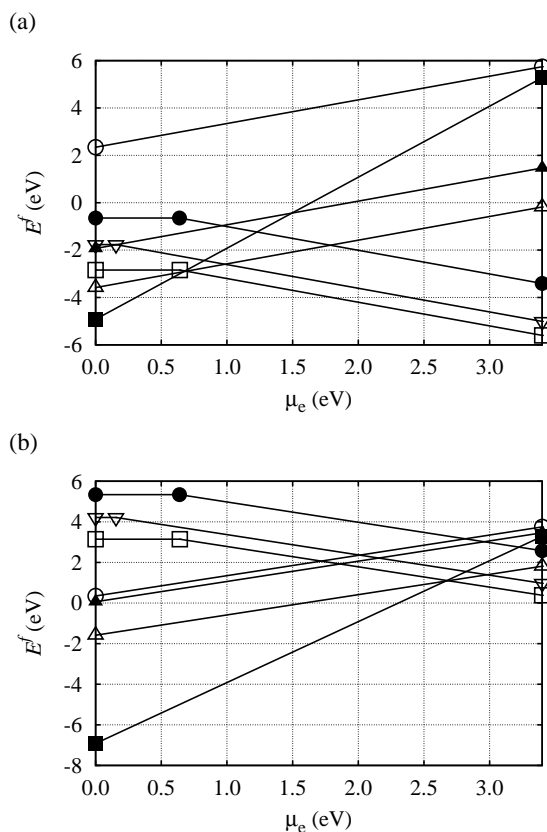


Fig. 8. Plot of E^f vs. μ_e for key P-containing defects in ZnO calculated using the 192 atom supercell: P_{Zn} (■), $P_{Zn}-(O_{int})_2$ (□), $P_{Zn}-(V_{Zn})_2$ (●), $P_{Zn}-O_{int}$ (△), $(PO)_O$ (○), $(PO_3)_O$ (▲), and $(PO_4)_O$ (▽). (a) Oxygen-rich conditions and (b) zinc-rich conditions

TABLE I
FORMATION ENERGIES PER IMPURITY IN O-RICH CONDITIONS FOR SELECTED GROUP-V AND GROUP-VI IMPURITIES IN COMPLEXES WITH V_{Zn} AND O_{int} IN ZnO, CALCULATED RELATIVE TO $X_{Zn}-(O_{int})_2$ (eV)

Defect	Impurity species, X				
	P	As	Sb	S	Se
X_{Zn}	4.2	3.0	3.1	3.8	4.1
$X_{Zn}-V_{Zn}$	2.2	2.7	2.8	3.4	2.8
$X_{Zn}-O_{int}$	1.2	1.4	1.4	1.7	1.1
$X_{Zn}-(V_{Zn})_2$	2.2	3.0	3.7	3.4	4.7
$X_{Zn}-V_{Zn}-O_{int}$	1.6	1.7	1.8	2.2	2.5
$(XO_4)_O$	0.9	3.6	3.6	0.5	3.6

Of particular importance is the thermal stability of the acceptor complexes. It has been determined that O_{int} is more mobile than V_{Zn} in ZnO [28], [56], having activation energies of 0.8 eV or less and 1.4 eV, respectively. Taking the activation for dissociation of complexes of P_{Zn} with V_{Zn} or O_{int} to be the sums of the binding energy and migration barriers for the native component, a simplistic model would lead to the reversal of p-type doping to be achieved at a lower temperature for O_{int} -based acceptors than for V_{Zn} -based centers. In addition, once $P_{Zn}-(O_{int})_2$ dissociates into $P_{Zn}-O_{int}+O_{int}$, the resultant components favor n-type material due to the amphoteric behavior of O_{int} . Then the type-dependence upon

growth temperature in P-doped films [57], [58] might be understood as the conversion of $P_{Zn}-(O_{int})_2$ acceptors into $P_{Zn}-O_{int}$, O_{int} and P_{Zn} -related donors.

The stabilizing effect of the formation of X–O bonds is also seen in the low formation energies of $(PO_4)_O$ shallow acceptors and $(SO_4)_O$ iso-electronic centers. In contrast, this type of structure centered upon As, Sb, or Se dopants are high in energy in comparison to the corresponding $X-(O_i)_2$ complexes. However, in these cases there is a substantial perturbation to the immediate neighbors, resulting in the displacement of a neighboring Zn atom. A small change in initial conditions for these complexes produce a $X_{Zn}(O_i)_2$ defect with a ZnO formula unit displaced into an interstitial location, which reduces the relative energies listed in Table I by around 1 eV. The balance of the formation energy is the cost of the formation of the self-interstitials. This may be viewed as further evidence that the production of acceptors in As and Sb doped materials might be correlated with the formation of six-fold oxygen-coordinated dopants.

IV. CONCLUSION

The overwhelming trend is for the group-V elements P, As, and Sb to adopt forms with multiple oxygen bonds, which result in both donor and acceptor configuration depending upon whether the material is under oxygen-rich or zinc-rich conditions.

We revise the previously favored structure of group-V acceptors involving native defects: the involvement of pairs of V_{Zn} in the formation of acceptor centers is energetically less favorable than the decoration with additional oxygen interstitials. However, the thermodynamic principle that acceptor species appear to be more likely to be formed in oxygen-rich conditions remains, since $P_{Zn}-(V_{Zn})_2$ and $P_{Zn}-(O_{int})_2$ depend upon μ_O in the same way.

Among the favored structures, the formation of coordinations between the dopants and more than four oxygen atoms may be resolvable experimentally, and we suggest that octahedral XO_5 and XO_6 structures are likely to have a wider impact: since the formation of these structures is largely driven by the strength of the impurity-oxygen bonds, doping of metal-oxides such as the high- κ dielectrics including TiO_2 and HfO_2 , and ferroelectric materials such as $BaTiO_3$ and $PbTiO_3$ with group-V and group-VI species is likely to result in these configurations.

REFERENCES

- [1] D. M. Bagnall, Y. F. Chen, Z. Zhu, T. Yao, S. Koyama, M. Y. Shen, and T. Goto, *Appl. Phys. Lett.* **70**, 2230 (1997).
- [2] Z. K. Tang, G. K. L. Wong, M. Yu, P. Kawasaki, A. Ohtomo, H. Koinuma, and Y. Segawa, *Appl. Phys. Lett.* **72**, 464 (1998).
- [3] D. K. Hwang, S. H. Kang, J. H. Lim, E. J. Yang, J. Y. Oh, J. H. Yang, and S. J. Park, *Appl. Phys. Lett.* **86**, 222101 (2005).
- [4] S. B. Zhang, S.-H. Wei, and A. Zunger, *Phys. Rev. B* **63**, 075205 (2001).
- [5] A. Kobayashi, O. F. Sankey, and J. D. Dow, *Phys. Rev. B* **28**, 946 (1983).
- [6] C. H. Park, S. B. Zhang, and S.-H. Wei, *Phys. Rev. B* **66**, 073202 (2002).
- [7] J. L. Lyons, A. Janotti, and C. G. Van de Walle, *Appl. Phys. Lett.* **95**, 252105 (2009).
- [8] S. Lany and A. Zunger, *Phys. Rev. B* **81**, 205209 (2010).
- [9] D. C. Look, D. C. Reynolds, C. W. Litton, R. L. Jones, D. B. Eason, and G. Cantwell, *Appl. Phys. Lett.* **80**, 1830 (2002).
- [10] Y. R. Ryu, T. S. Lee, and H. W. White, *Appl. Phys. Lett.* **83**, 87 (2003).
- [11] J. M. Bian, X. M. Li, C. Y. Zhang, W. D. Yu, and X. D. Gao, *Appl. Phys. Lett.* **85**, 4070 (2004).
- [12] A. Tsukazaki, A. Ohtomo, T. Onuma, M. Ohtani, T. Makino, M. Sumiya, S. F. Ohtani, K. Chichibu, S. Fuke, Y. Segawa, H. Ohno, H. Koinuma, and M. Kawasaki, *Nature Mater.* **4**, 42 (2005).
- [13] Y. R. Ryu, T. S. Lee, J. H. Leem, and H. W. White, *Appl. Phys. Lett.* **83**, 4032 (2003).
- [14] K.-K. Kim, H.-S. Kim, D.-K. Hwang, J.-H. Lim, and S.-J. Park, *Appl. Phys. Lett.* **83**, 63 (2003).
- [15] F. X. Xiu, Z. Yang, L. J. Mandalapu, D. T. Zhao, and J. L. Liu, *Appl. Phys. Lett.* **87**, 252101 (2005).
- [16] F. X. Xiu, Z. Yang, L. J. Mandalapu, D. T. Zhao, and J. L. Liu, *Appl. Phys. Lett.* **87**, 252102 (2005).
- [17] A. Allenic, W. Guo, Y. B. Chen, Y. Che, Z. D. Hu, B. Lu, and X. Q. Pan, *J. Phys. D* **41**, 025103 (2008).
- [18] G. Xiong, J. Wilkinson, B. Mischuck, S. Tüzemen, K. B. Ucer, and R. T. Williams, *Appl. Phys. Lett.* **80**, 1195 (2002).
- [19] Y. W. Heo, K. Ip, S. J. Park, S. J. Pearton, and D. P. Norton, *Appl. Phys. Lett.* **78**, 53 (2004).
- [20] S. Limpijumnong, S. B. Zhang, S.-H. Wei, and C. H. Park, *Phys. Rev. Lett.* **92**, 155504 (2004).
- [21] W.-J. Lee, J. Kang, and K. J. Chang, *Phys. Rev. B* **73**, 024117 (2006).
- [22] D. E. Pugal, R. D. Vispute, S. S. Hullavarad, T. Venkatesan, and B. Varughese, *J. Appl. Phys.* **101**, 063538 (2007).
- [23] U. Wahl, J. G. Correia, T. Mendonça, and S. Decoster, *Appl. Phys. Lett.* **94**, 261901 (2009).
- [24] U. Wahl, E. Rita, J. G. Correia, A. C. Marques, E. Alves, J. C. Soares, and ISOLDE Collaboration, *Phys. Rev. Lett.* **95**, 215503 (2005).
- [25] J. M. Qin, B. Yao, Y. Yan, J. Y. Zhang, X. P. Jia, Z. Z. Zhang, B. H. Li, C. X. Shan, and D. Z. Shen, *Appl. Phys. Lett.* **95**, 022101 (2009).
- [26] J. Hu and B. C. Pan, *J. Chem. Phys.* **129**, 154706 (2008).
- [27] P. Erhart, K. Albe, and A. Klein, *Phys. Rev. B* **73**, 205203 (2006).
- [28] A. Janotti and C. G. Van de Walle, *Phys. Rev. B* **76**, 165202 (2007).
- [29] P. R. Briddon and R. Jones, *Phys. Status Solidi B* **217**, 131 (2000).
- [30] M. J. Rayson and P. R. Briddon, *Computer Phys. Comm.* **178**, 128 (2008).
- [31] H. J. Monkhorst and J. D. Pack, *Phys. Rev. B* **13**, 5188 (1976).
- [32] N. Troullier and J. L. Martins, *Phys. Rev. B* **43**, 1993 (1991).
- [33] J. P. Perdew and Y. Wang, *Phys. Rev. B* **45**, 13244 (1992).
- [34] J. P. Goss, M. J. Shaw, and P. R. Briddon, in *Theory of Defects in Semiconductors*, Vol. 104 of *Topics in Applied Physics*, edited by David A. Drabold and Stefan K. Streicher (Springer, Berlin/Heidelberg, 2007), pp. 69–94.
- [35] M. J. Rayson and P. R. Briddon, *Phys. Rev. B* **80**, 205104 (2009).
- [36] *CRC handbook of chemistry and physics*, 73 ed., edited by D. R. Lide (CRC, Boca Raton, FL, 1992).
- [37] S. Lany and A. Zunger, *Phys. Rev. B* **78**, 235104 (2008).
- [38] We do not include nitrogen in this study as the chemistry of this species is distinct from that of the larger main-group elements. A study of the comparable systems involving N is in preparation.
- [39] Z. G. Yu, H. Gong, and P. Wu, *Appl. Phys. Lett.* **86**, 212105 (2005).
- [40] R.-Y. Tian and Y.-J. Zhao, *J. Appl. Phys.* **106**, 043707 (2009).
- [41] C. H. Park, S. B. Zhang, and Su-Huai Wei, *Phys. Rev. B* **66**, 073202 (2002).
- [42] Since the composition of these centers differs by one Zn and one O atom, the difference in the formation energies is independent of μ_O .
- [43] R. Qin, J. Zheng, J. Lu, L. Wang, L. Lai, G. Luo, J. Zhou, H. Li, Z. Gao, G. Li, and W. N. Mei, *J. Phys. Chem. C* **113**, 9541 (2009).
- [44] J. Dong, A. A. Kinkhabwala, and P. F. McMillan, *Phys. Scr.* **10**, 2319 (2004).
- [45] F. Brunet, A.-M. Flank, J.-P. Itié, T. Irifune, and P. Lagarde, *Am. Miner.* **92**, 989 (2007).
- [46] N. V. Timosheva, A. Chandrasekaran, R. O. Day, and R. R. Holmes, *Inorg. Chem.* **37**, 3862 (1998).
- [47] D.-K. Hwang, H.-S. Kim, J.-H. Lim, J.-Y. Oh, J.-H. Yang, S.-J. Park, K.-K. Kim, D. C. Look, and Y. S. Park, *Appl. Phys. Lett.* **86**, 151917 (2005).
- [48] X. Xu, Y. Shen, N. Xu, W. Hu, J. Lai, Z. Ying, and J. Wu, *Vacuum*, in press, 2010.
- [49] V. Vaithianathan, K. Asokan, J. Y. Park, and S. S. Kim, *Appl. Phys. A* **94**, 995 (2009).
- [50] W. Y. Ching and P. Rulis, *Phys. Rev. B* **77**, 125116 (2008).
- [51] J. Pellicer-Porres, A. M. Saitta, A. Polian, J. P. Itié, and M. Hanfland, *Nature Mater.* **6**, 698 (2007).
- [52] S. D. Perez, J. Haines, U. Amador, E. Moran, and A. Vegas, *Surface Sci.* **62**, 1019 (2006).

- [53] F. Brunet, A.-M. Flank, Itie J.-P., T. Irifune, and P. Lagarde, *Adv. Mat.* **92**, 989 (2007).
- [54] A. B. Padmaperuma, L. S. Sapochak, and P. E. Burrows, *Chem. of Materials* **18**, 2389 (2006).
- [55] The case of N is quite different, with structures formed resembling common N-O molecular species, which will be the subject of a future paper.
- [56] P. Erhart and K. Albe, *Phys. Rev. B* **73**, 115207 (2006).
- [57] B. Claflin, D. C. Look, S. J. Park, and G. Cantwell, *J. Cryst. Growth* **287**, 16 (2006).
- [58] G. Hu and H. Gong, *Acta Mater.* **56**, 5066 (2008).